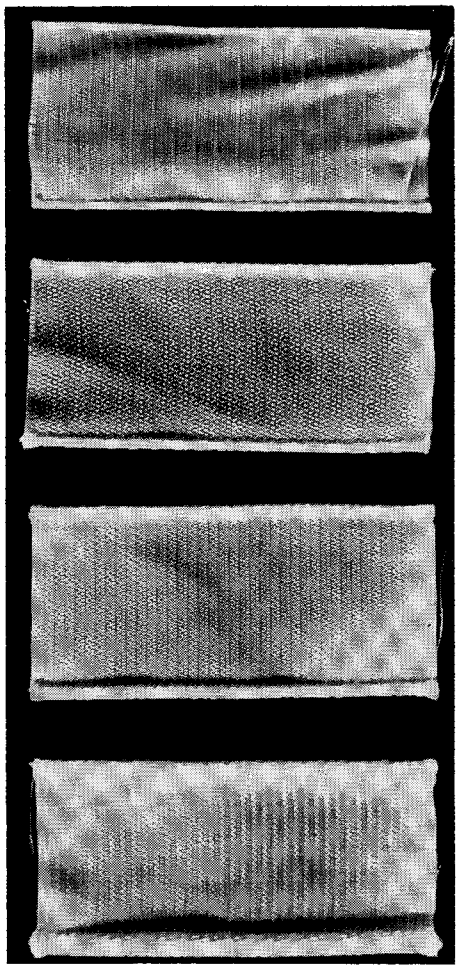

Fig. 3 Reinforced selvage ribbon—from top to bottom are shown 1000-, 2000-, 3000-, and 4000-lb tensile strength.

was adequate to slow the vehicle down rapidly; and disreefing allowed the chute to go full open so the impact velocity would be low enough to allow the nose-spike to penetrate the ground and leave the vehicle standing upright, as shown in Fig. 5.

Conclusions

A series of nine Nike rocket-boosted parachute tests have been conducted from which the following conclusions can be drawn: 1) The specially designed 20-ft-diam ribbon parachute can be used to recover a 1100-lb payload up to a Mach number of 2.2 and a dynamic pressure of 4300 psf. 2) The new reinforced selvage ribbon has been instrumental in perfecting parachutes that will operate in the environment previously described.

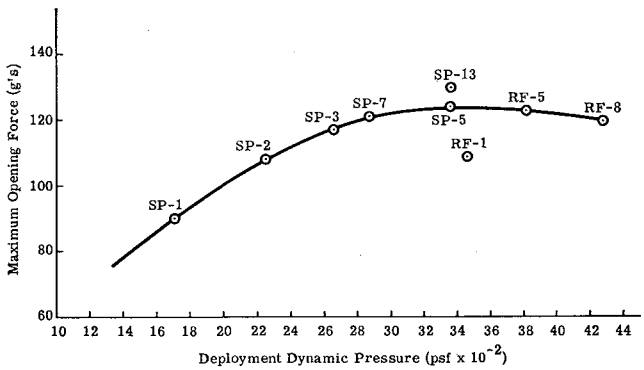

Fig. 4 Variation of maximum opening force with dynamic pressure.

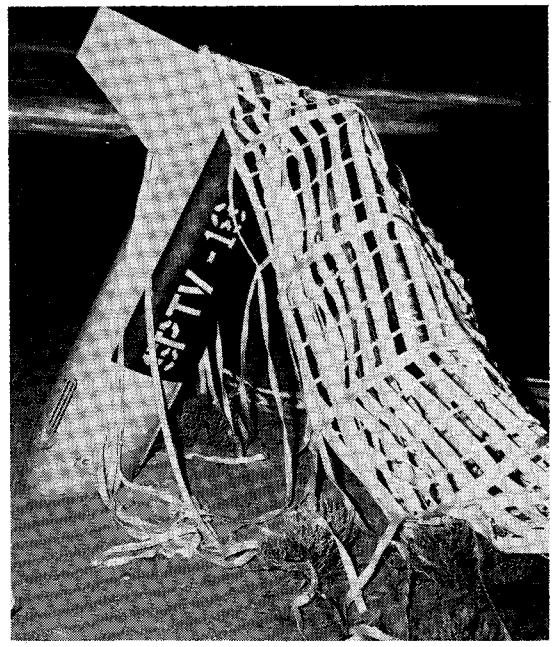

Fig. 5 Vehicle and 20-ft-diam parachute after successful test at Tonopah Test Range, Nev.

Reference

[1] Kane, M. T., "Design and testing of a 20-foot-diameter ribbon parachute for deployment at high dynamic pressures," Sandia Corp., SC-RR-66-79 (April 1966).

Determination of Subsonic Drag Rise by Hodograph Plane Analysis

M. S. Cahn* and G. M. Andrew†
Northrop Norair, Hawthorne, Calif.

Introduction

Previous work by Piercey[1] has shown that the drag divergence Mach number for an airfoil can be determined by studying the conditions at the crestline of the section. However, the physical significance of the crestline rule of thumb remains vague. The importance of the crestline was discovered by British workers from examination of plots of pressure coefficient vs Z (vertical distance) rather than the usual presentation of pressure coefficient vs percent chord.

It now seems that a hodograph representation may give a better understanding of the conditions for the formation of a strong shock or drag divergence. It can be shown that the conditions for the existence of flow breakdown can be determined from the hodograph plane. Where a decelerating streamline becomes tangent to the characteristic lines in the hodograph plane, steady isentropic flow will break down and a limit line will exist.

A study of this hodograph analysis suggested a direct method for transonic airfoil design. These concepts seem able to explain the physics of the crestline rule. Also indicated is the possibility of using large trailing edge angles with boundary-layer control to prevent separation.

Submitted December 28, 1966; also presented as Paper 67-4 at the AIAA 5th Aerospace Sciences Meeting, New York, January 23–26, 1967. [3.02]

* Research Aerodynamicist. Member AIAA.
† Research Aerodynamicist. Associate Fellow AIAA.

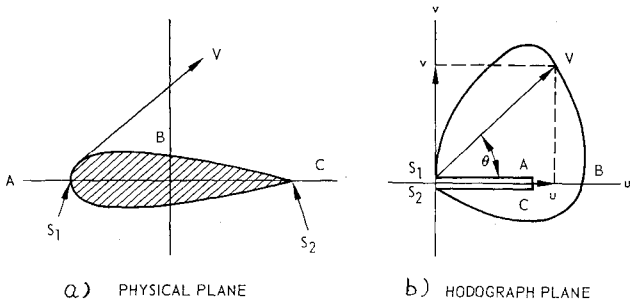

Fig. 1 Flow around an airfoil.

To substantiate this concept, pressure data for several NACA airfoils were plotted in hodograph form. The theoretically obtained Mach number for drag rise was compared with the value obtained from the wind tunnel. This comparison shows excellent correlation. The results of this study indicate that airfoil design and improvement techniques can be developed by the hodograph analysis.

Description of Hodograph Plane

The most promising method of solving mixed subsonic and supersonic flows around bodies is by use of the hodograph transformation. This method was first introduced in 1890 by Molenbroeck[2] and by Chaplygin in 1904.[3] A complete discussion of the hodograph method is presented by Lighthill[4] and by Garrick and Kaplan.[5] The flow equations in the hodograph plane have been the basis for almost all of the useful transonic correction factors.

The word "hodograph" (from the Greek hodos or path plus graph or line) is used to refer to a representation where any point represents the extremity of the velocity vector at a point in the physical plane. A simpler way of stating this is that the vertical axis represents the magnitude of the vertical velocity component, and the horizontal axis represents the magnitude of the horizontal velocity component. An alternate name for this representation is velocity plane.

Consider the flow about a symmetrical airfoil (Fig. 1a). The flow approaches from freestream velocity at infinity on the left, slows down, and comes to rest at the front stagnation point. The flow then turns 90° and accelerates as it flows around the airfoil to the rear stagnation point. The hodograph of this flow is shown in Fig. 1b. Note that the curve

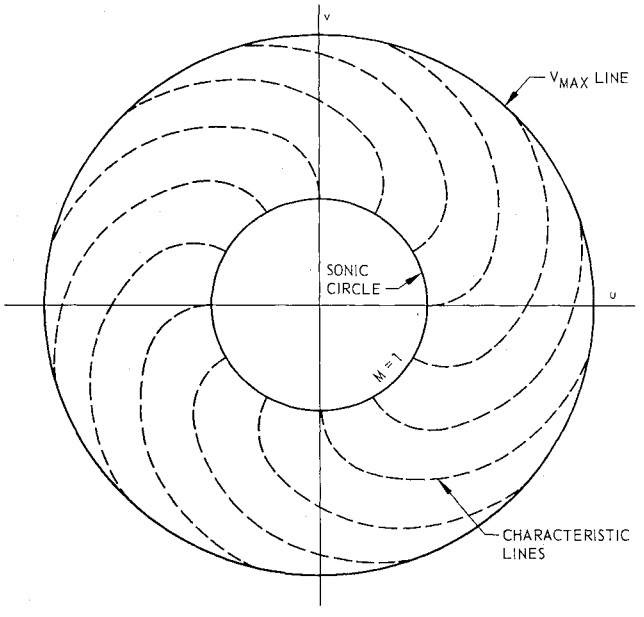

Fig. 2 Characteristic lines of one family in hodograph plane.

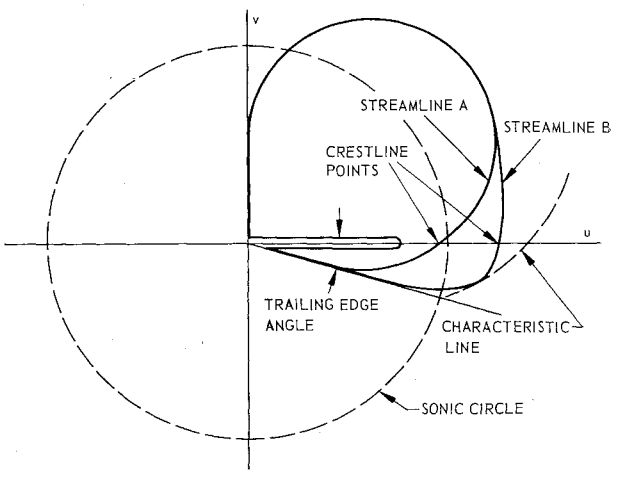

Fig. 3 Illustration of crestline rule.

shown is for the upper surface only. The lower surface, which is not shown, is on another plane connected to the illustrated plane through the branch cut AS_1 and CS_2.

The principal advantage of the hodograph equations is that they are linear in the dependent variable ψ, the stream function. Therefore, the equations can be solved in the hodograph plane and solutions can be added.

Generally the principal disadvantage is that boundary conditions in the physical plane cannot be described in the hodograph plane. However, in this paper it is suggested that a satisfactory shock-free boundary condition can be described in the hodograph plane. This boundary condition can then be satisfied with the hodograph equations, and the geometry of the airfoil in the physical plane can be determined.

Limit Line

When a flow is described in the hodograph plane and then transformed to the physical plane, discontinuities often appear which did not exist in the hodograph plane. The streamlines in the physical plane form cusps that would require infinite accelerations. Since this is impossible in real flow, it is generally recognized that one of the assumptions of steady isentropic flow breaks down. Experience indicates that shock waves are formed in the physical plane where limit lines exist. It can be shown that a criterion for the existence of a limit line can be determined in the hodograph plane. This criterion is stated in Shaprio[6] as follows: "At a point on the hodograph limit line the hodograph streamline is locally tangent to the hodograph characteristics of one family." The two families of characteristic lines are each an infinite set of epicycloids starting at the sonic line. One family is shown in Fig. 2 (the other family is a mirror image).

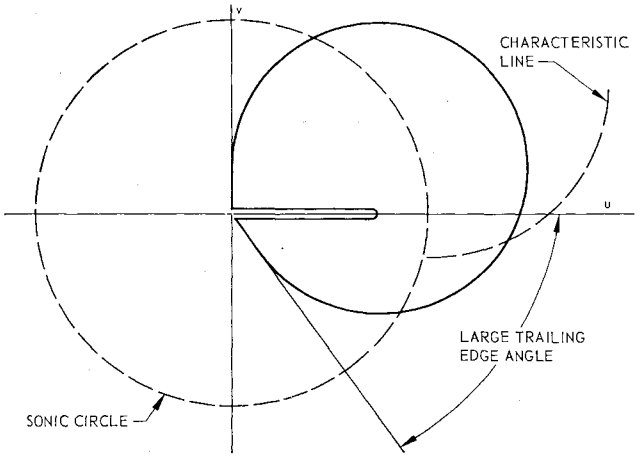

Fig. 4 Hodograph streamline for airfoil with large trailing edge angle.

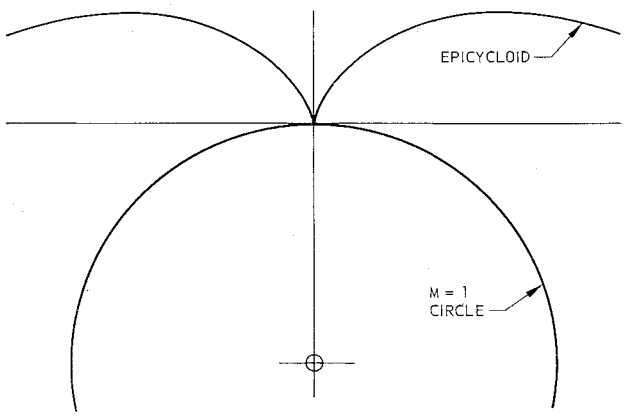

Fig. 5 Characteristic line underlay.

Some Transonic Airfoil Rules from the Hodograph Analysis

At this point the hodograph analysis can be used to illustrate some well-known rules for transonic airfoils. Note in Fig. 3 that the crestline is the point where the hodograph streamline crosses the horizontal axis. If the hodograph streamline becomes subsonic near the crestline (see streamline A), it can then turn around and go to the rear stagnation point (at the origin in Fig. 3) at a reasonable trailing edge angle without becoming tangent to a characteristic line. If the streamline remains supersonic beyond the crestline (see streamline B), it must turn sharply to meet the trailing edge angle and will necessarily become tangent to a characteristic line. The accelerating portion of the streamline can probably be tangent to the characteristic lines and cause harmless limit lines that are enclosed within the body. An example of this is Prandtl-Meyer accelerating flow around a corner.

If the trailing edge angle is increased, as shown in Fig. 4, the streamline can remain supersonic for larger flow angles and still not violate the limit line criterion. This suggests the possibility of large trailing edge angles for transonic flow if a means of preventing separation by some form of boundary-layer control can be achieved.

Experimental Verification

Experimental data were used to test the possible usefulness of the limit line criterion for airfoil design. The data were taken from Stivers,[7] where pressure coefficients and drag data for four NACA airfoils (64A Series) are given. The airfoils were tested at various angles of attack (0°–10°) throughout the Mach number range from 0.41 to 0.93. The pressure coefficients were converted to the ratio of local velocity to the sonic speed of sound, V/a^*. These velocity ratios were plotted in polar form with the flow inclination angle θ as the angular

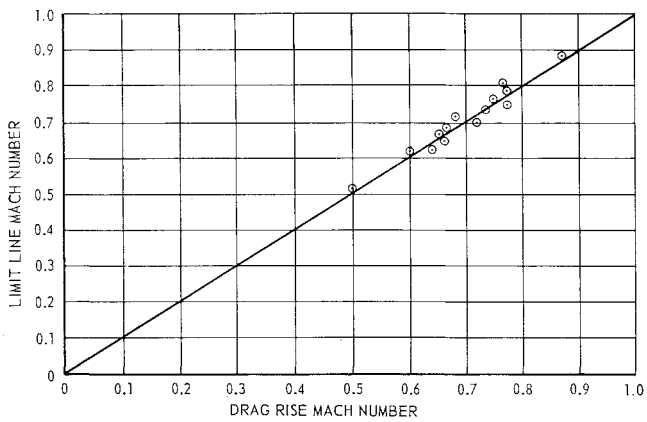

Fig. 6 Comparison of limit line and drag divergence Mach number.

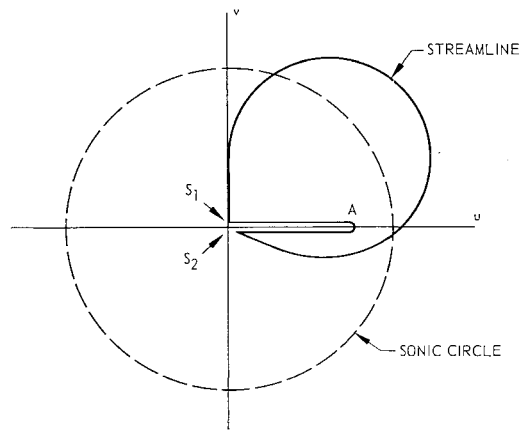

Fig. 7 Airfoil design in hodograph plane.

variable, thus forming a hodograph representation of the flow. The epicycloids of both families were plotted on another sheet (Fig. 5) which could be placed under the hodograph of the flow. The upper sheet was rotated to determine if the airfoil streamline was anywhere tangent to the characteristic lines. The Mach number at which tangency first occurred was noted. Only the decelerating portion of the streamline was used; this portion was always tangent to the same family of characteristic lines. The drag divergence Mach number was determined from drag coefficient vs Mach number plots in Ref. 7. The drag divergence Mach number was then plotted vs the limit line Mach number and is shown in Fig. 6. Excellent correlation is indicated in this figure.

Method for Design of Transonic Airfoil

The preceding discussion of the hodograph equations and limit line criterion suggests a direct method for transonic airfoil design. First a streamline is drawn in the hodograph plane (see Fig. 7). The freestream velocity at infinity is satisfied at point A. The velocity remains horizontal and slows down to zero at the front stagnation point, turns 90°, and flows around the airfoil, becoming supersonic and decelerating without being tangent to any of the characteristic epicycloids.

Once this boundary is determined, the hodograph equations of motion that satisfy the given boundary conditions are satisfied. From this the coordinates of the airfoil section in the physical plane could be determined.

The solution of the hodograph equations to fit arbitrary boundary conditions is being studied now at Northrop Norair. Much work on this problem was accomplished many years ago. Modern high-speed computing machines now make actual solutions possible.

Conclusion

Useful information may be obtained if hodograph plots are used during the design and testing of transonic airfoils. If a wind-tunnel test of a series of airfoils is conducted, as is often done for many of today's designs, the experimental results in hodograph form would assist in understanding the drag rise. This should even suggest improvements to the shape which would produce a higher drag rise Mach number.

With the availability of modern computational techniques it is believed that methods can be developed for solution of the hodograph flow equations for arbitrary boundary conditions. By designing properly in the hodograph plane, the geometry of airfoil sections having a drag rise at higher Mach numbers could be obtained. Northrop Norair is currently studying this problem.

References

[1] Piercey, H. H., "The aerodynamic design of section shapes for swept wings," *Proceedings of the Second International Congress*

in the Aeronautical Sciences (The Macmillan Company, New York, 1962), Vol. 3, pp. 277–322.

[2] Molenbroeck, P., "Uber einige Bewegungen eines Gases mit Annahme eines Geschwindigkeits-potentials," Arch. Math. Phys. **9**, 157–195 (1890).

[3] Chaplygin, S. A., "On gas jets," Sci. Ann., Moscow Imperial Univ., Math–Phys. Sec. **21**, 1–121 (1904); also NACA TM 1063 (1944).

[4] Lighthill, M. J., "The hodograph transformation in transonic flow," Proc. Roy. Soc. (London) **A191**, 323, 341, 352 (1947); Proc. Roy. Soc. (London) **A192**, 135 (1947).

[5] Garrick, I. E. and Kaplan, C., "On the flow of a compressible fluid by the hodograph method: II—fundamental set of particular flow solutions of the Chaplygin differential equation," NACA TR 790 (1944).

[6] Shapiro, A. H., *The Dynamics and Thermodynamics of Compressible Fluid Flow* (Ronald Press Company, New York, 1954), Vol. II.

[7] Stivers, L. S., Jr., "Effects of subsonic Mach number on the force and pressure distribution on four NACA 64A-series airfoil sections at angles of attack as high as 28°," NACA TN 3162 (March 1964).

Alternate Approach for Aerospacecraft Design Sensitivities

HUGO P. HEERMANN* AND JOHN S. CLAUSS JR.†
Lockheed-California Company, Burbank, Calif.

IN Ref. 1, the classical indirect method of the calculus of variations is used to determine the optimum performance for a vehicle of given design. In Ref. 2, this work is extended by treating design variables as special control variables, and a fundamental variational relation of Leitmann[3] is used to deduce tradeoff relations or sensitivities between the performance index and the design variables. The purpose of this note is to offer an alternate approach to the derivation of these sensitivities.

Classical Variational Problem

Reference 1 considers the problem of determining the control variable histories

$$u_j(t) \qquad j = 1, 2, \ldots n \tag{1}$$

and the state variable histories

$$x_i(t) \qquad i = 1, 2, \ldots m \tag{2}$$

subject to the satisfaction of the differential equations

$$\dot{x}_i = f_i(t, x_i, u_j) \qquad i = 1, 2, \ldots m \qquad j = 1, 2, \ldots n \tag{3}$$

and the end conditions

$$\Psi_r[t^i, t^f, x_i(t^i), x_i(t^f)] = 0 \qquad r = 1, 2, \ldots q < 2m + 2 \tag{4}$$

in order to minimize a given performance index

$$G[t^i, t^f, x_i(t^i), x_i(t^f)] \tag{5}$$

The solution to this problem is secured by introducing m Lagrange multipliers

$$\lambda_1, \lambda_2 \ldots \lambda_m \tag{6}$$

and defining the generalized Hamiltonian by

$$H = \sum_{i=1}^{m} \lambda_i f_i \tag{7}$$

An optimum trajectory must satisfy the Euler-Lagrange equations

$$\dot{x}_i = \partial H/\partial \lambda_i \tag{8}$$

$$\dot{\lambda}_i = \partial H/\partial x_i \qquad (i = 1, 2, \ldots m) \tag{9}$$

$$0 = \partial H/\partial u_j \qquad (\ = 1, 2, \ldots n) \tag{10}$$

and the transversality condition

$$\left[-H(t^s)dt^s + \sum_{i=1}^{m} \lambda_i(t^s)dx_i(t^s)\right]_{s=i}^{s=f} + dG = 0 \tag{11}$$

where (11) must hold for all sets of differentials

$$dt^i, dx_i(t^i), dt^f, dx_i(t^f) \qquad i = 1, 2, \ldots m \tag{12}$$

which satisfy

$$d\Psi_r = 0 \qquad r = 1, 2, \ldots q \tag{13}$$

The system composed of the constraining equations (4) and the Euler-Lagrange equations (8–10) is subject to $2m + 2$ boundary conditions for the optimum choice of the $2m + 2$ initial and final variables

$$t^i, t^f, x_i(t^i), x_i(t^f) \qquad i = 1, 2, \ldots m$$

Of these, q are supplied by (4) and the remaining $2m + 2 - q$ are supplied by the transversality conditions (11–13). The maximum number of restraints [Eq. (4)] that can be considered is $2m + 1$. In this latter case, one free variable is left to be determined from the transversality condition.

Fundamental Formula

If J denotes the minimum value of G subject to the given end conditions [Eq. (4)], then the formula of Leitmann[3]‡ is given by

$$dJ = dG + \left[-H^s dt^s + \sum_{i=1}^{m} \lambda_i(t^s)dx_i(t^s)\right]_{s=i}^{s=f} - \int_{t^i}^{t^f} \sum_{j=1}^{n} \frac{\partial H}{\partial u_j}\,\delta u_j\,dt \tag{14}$$

Along an optimum path, $dJ = 0$. The last term in (4) vanishes because of Eq. (10), and the first two terms combine with the given end conditions [Eq. (13)] to make $dJ = 0$.

Once an optimum path has been obtained, one may now go back and examine (14) to see what effect small perturbations on one or more of the state variables will have on J. To this end, Leitmann[3] assumes that the end values t^i, t^f, $x_\rho(t^i)$, $x\rho(t^f)$, $1 \leq \rho \leq m$, do not occur in G or the end conditions [Eq. (4)], and then calculates the effects of small perturbations

$$t^i + dt^i \qquad t^f + dt^f \qquad x_\rho(t^i) + dx_\rho(t^i) \qquad x_\rho(t^f) + dx_\rho(t^f)$$

on the performance index. In particular, because of (10) and (11), all terms of the right member of (14) vanish except those containing dt^i, dt^f, $dx_\rho(t^i)$, $dx_\rho(t^f)$. Thus (14) becomes

$$dJ = -H(t^f)dt^f + H(t^i)dt^i + \lambda_\rho(t^f)dx_\rho{}^f - \lambda_\rho(t^i)\,dx_\rho{}^i \tag{15}$$

and as a consequence one deduces that

$$\partial J/\partial t^f = -H(t^f) \qquad \partial J/\partial t^i = H(t^i) \tag{16}$$

$$\partial J/[\partial x_\rho(t^i)] = -\lambda_\rho(t^i) \qquad \partial J/[\partial x_\rho(t^f)] = \lambda_\rho(t^f) \tag{17}$$

Received March 13, 1967. [2.04]

* Mathematical Specialist. Member AIAA.

† Flight Sciences Methods Group Engineer. Associate Fellow AIAA.

‡ For simplicity we exclude the case where the trajectory has corner points. Also, there are no equality nor inequality restraints on t, x_i, u_j.